

Modeling of Stress Evolution of Electroplated Cu Films during Self-annealing

Rui Huang

Kompetenzzentrum Automobil-und Industrieelektronik (KAI) GmbH

Europastrasse 8, 9524 Villach, Austria

0043-4242-34890-16, rui.huang@k-ai.at

Werner Robl

Infineon Technologies AG

Wernerwerkstrasse 2, 93049 Regensburg, Germany

Thomas Detzel

Infineon Technologies Austria AG

Siemensstrasse 2, 9500 Villach, Austria

Hajdin Ceric

Institute for Microelectronics, TU Wien

Gusshausstrasse 27-29, 1040 Vienna, Austria

Abstract—Electroplated Cu films are known to change their microstructure at room temperature due to the self-annealing effect. This recrystallization process results in a film-thickness-dependent stress evolution. Films with the thickness of 5 μ m and below decrease in stress with time, while thicker films reveal initially an increase in film stress followed by a stress relaxation at a later stage. This behavior is explained by the superposition of grain growth and grain size dependent yielding. Existing models have been used and improved to describe the mechanisms related to stress evolution. In general, the models proposed in this study provide a satisfactory description of the stress evolution of electroplated Cu films and the simulated results show good agreement with the experimental data. This gives the possibility to evaluate and predict mechanical behavior of electroplated Cu films at room temperature.

Keywords-modeling; stress; Cu films; self-annealing

I. INTRODUCTION

Copper has replaced aluminum for interconnect applications in semiconductor devices due to its higher electrical conductivity, increased electromigration resistance and better thermal conductivity [1]. Electro-chemical deposition (ECD) of copper has been demonstrated as one of the best methods to be adopted for high performance logic devices using dual damascene technology and for power devices using pattern plating technology [2-4]. The recrystallization of ECD Cu at room temperature, which is termed self-annealing, is a very distinct phenomenon [5-8]. During self-annealing, stress change is observed [7-11], which is associated with a transition from an as-deposited ultrafine-

This work was jointly funded by the Federal Ministry of Economics and Labor of the Republic of Austria (contract 98.362/0112-C1/10/2005 and the Carinthian Economic Promotion Fund (KWF) (contract 18911 | 13628 | 19100).

grained microstructure to a coarse-grained microstructure. It may require expensive post deposition treatments to overcome the self-annealing which might cause reliability impairment. Thus, the control of stress development is of great importance to ensure the lifetime and reliability performance of Cu metallization.

So far, most of the research has been devoted to analyze mechanisms and kinetics of self-annealing of ECD Cu films [5, 9, 12-18]. Only very few publications can be found which present the modeling results regarding the self-annealing effect. Still, most of them only focus on the modeling in terms of sheet resistivity evolution [19, 20]. The purpose of the present work is to develop a model which is able to describe the mechanisms of stress evolution of ECD Cu films based on experimental studies published elsewhere [21] so that the prediction of the stress evolution at room temperature becomes feasible.

II. EXPERIMENTAL OBSERVATIONS

The film stress of electroplated Cu films with the thickness between 1.5 and 20 μ m was measured at room temperature by the time elapsed. As illustrated in Fig. 1, all films show a tensile stress. Thin Cu films (1.5-5 μ m) have relatively high initial stress compared to thick Cu films (8-20 μ m). The stress evolution shows a disparate tendency between these two groups: i) thin films with the thickness of 5 μ m and below, ii) thick films with the thickness of 8-20 μ m. The as-deposited film stress shows also an inverse relationship between film stress and film thickness. The tensile stress of thin films continues to decrease with time, while for thick Cu films the stress first

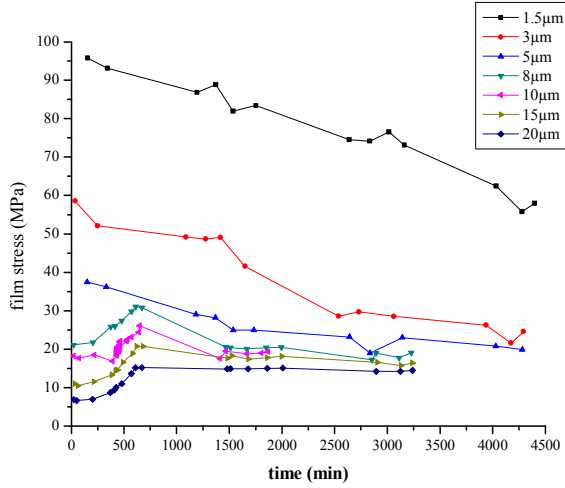


Figure 1. Stress evolution of 1.5-20 μm thick Cu films at room temperature. Disparate tendencies of stress are observed between thin Cu films (1.5-5 μm) and thick Cu films (8-20 μm).

increases and subsequently starts to decrease or stagnate depending on the maximum stress value. Finally, the tensile stress values of all Cu films stagnate at a certain value, which is determined by the film thickness. Thicker films reveal a lower final stress than thinner films.

Meanwhile, the images in Fig. 2 made by focused ion beam (FIB) technique show a remarkable grain growth of 8 μm thick Cu film during self-annealing. The first FIB image taken 2h after deposition reveals a fine globular grain structure. After 20h, a significant change in grain size has occurred. The grains which frequently contain twins have a bimodal grain size distribution. It should be noted, that at the Cu/substrate interface, a ~300nm thick region of fine grains still exists. After 44h, all fine grains have been consumed by large grains. Some of the grains (columnar grains) extend through the complete thickness of the film and contain twins. The coexistence of columnar grains and twins leads again to a bimodal grain size distribution. With the help of the linear intercept method, average grain size can be calculated based on each FIB image. Twins are counted as grains. The 45° tilt angle of the FIB images has been taken into account for the grain size analysis. The average grain sizes of 8 μm thick Cu film are approximately 135nm, 210nm and 290nm according to the FIB images taken after 2h, 20h and 44h at room temperature, respectively.

The observed stress evolution of ECD Cu films can be explained by the superposition of grain growth and grain size

dependent yielding. On the one hand, grain growth leads to annihilation of excess film volume by reducing the amount of grain boundaries. This gives rise to the stress increase in tension due to the shrinkage of the film volume if the film remains bonded to the substrate. On the other hand, dislocation plasticity leads to the stress decrease by relaxing the film. When initial stress is high, dislocation glide acts as the dominant mechanism and overtakes the effect of grain growth. Thereby it exhibits the continuous stress decrease in Cu films with the thickness of 1.5-5 μm . When initial stress is low such as in the case of Cu films with the thickness of 8-20 μm , dislocation glide cannot be activated immediately. Instead, grain growth plays a dominant role in the early stage of stress evolution. Until film stress reaches a threshold value, dislocation plasticity is then triggered. Afterwards, the stress decreases like in the 8 and 10 μm thick Cu films when the effect of dislocation plasticity becomes more prominent than that of grain growth. For the 15 and 20 μm thick films the peak stresses are still so low that dislocation glide and grain growth counterbalance each other. As a consequence, stress evolution of ECD Cu films ascribes to the competing mechanisms of grain growth and dislocation plasticity.

III. MODEL

A. Stress increase due to the loss of grain boundary volume

The loss of grain boundary volume due to grain growth induces the shrinkage of the film volume. If the film remains constrained to the substrate, it causes stress increase in tension. Chaudhari has presented a model which explains the stress development due to grain growth [8, 22]. It calculates the strain in the film by estimating the change in volume associated with the coalescence of grain boundaries. The density of a region containing a grain boundary is usually lower than that of a region containing no boundary. Assuming a grain boundary parameter α ($0 < \alpha < 1$), the boundary region has the same density as the grain if $\alpha = 0$, and a monolayer of atoms is missing in the boundary if $\alpha = 1$. Hereby the grain boundary

parameter α can be defined as $\alpha = \frac{w - a}{a}$ in terms of the grain boundary width w and the atomic diameter a . When grain growth starts, two boundaries coalesce to generate a single boundary. Thus, the elastic distortion in the film due to grain growth can be given by $2w - (w + a) = w - a = \alpha a$.

Considering a thin film that has an average grain size L_0 in the as-deposited condition, and assuming the grains grow to final grain size L , the total elastic strain associated with grain

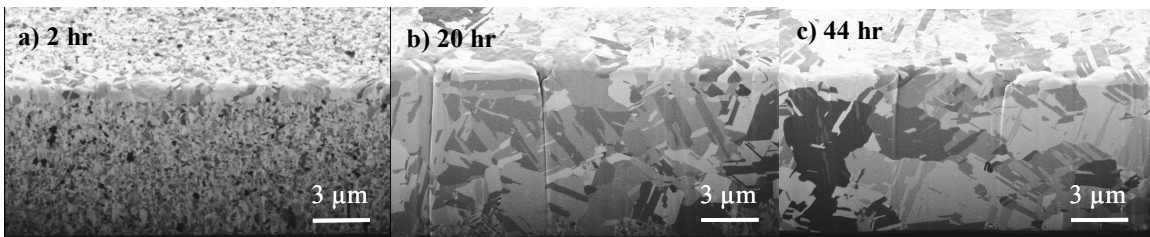


Figure 2. Microstructural evolution of 8 μm thick Cu film at room temperature. a). 2 hours after deposition only fine grains are existing in the film; b). 20 hours after deposition coarse grains are formed while fine grains are still existing at the bottom of the film; c). 44 hours after deposition, coarse grains occupy the film, where twins are embedded.

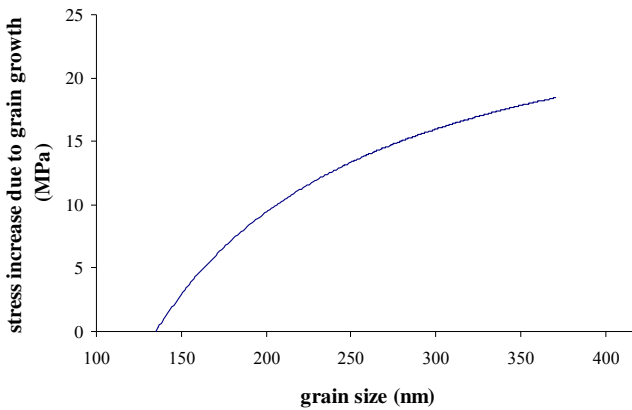


Figure 3. Stress increase due to grain growth, calculated by Chaudhari's model [22]. Original grain size is 135nm. ($E=121\text{GPa}$, $v=0.33$)

growth is [22]

$$\Delta\epsilon_{gg} = \frac{\alpha a}{2} \left(\frac{1}{L_0} - \frac{1}{L} \right) \quad (1)$$

Then the total change of biaxial stress associated with grain growth is given by

$$\Delta\sigma_{gg} = \frac{E}{1-v} \Delta\epsilon_{gg} = \frac{E}{(1-v)} \frac{\alpha a}{2} \left(\frac{1}{L_0} - \frac{1}{L} \right) \quad (2)$$

where $\Delta\sigma_{gg}$ is the stress increase induced by grain growth, E is the elastic modulus of the film, v is the Poisson's ratio of the film, and a is the bulk atom layer spacing (0.36148nm) [8].

If it is assumed that original and final grain size are 135 and 370nm, respectively, the total stress increase calculated is about 25MPa which is plotted in Fig. 3. It must be pointed out that the value of the grain boundary parameter α can vary with the deposition conditions, such as electrolyte composition or current density [23]. Moreover, grain growth and coalescence of grain boundaries are not homogeneous over the film, as seen in Fig. 2. It is very difficult to set the global α value accurately based on the actual local values over the film. In our model, it is assumed that α is the average over transformed and untransformed grains and it is estimated to be 0.12 based on the best fitting, which is fairly close to the value of 0.15 found by Cabral [24].

B. Grain growth rate

As Chaudhari's model describes stress evolution as function of grain size, it additionally needs an intermediate model which introduces the grain size development as function of time elapsed so that the stress evolution can be correlated with time. Doerner and Nix have successfully developed such a grain growth model to describe the rate of grain size development [25].

There are two major contributions to the total energy E_{total} of a film during grain growth. One is the grain boundary energy E_{gb} , and another is the elastic strain energy W_{el} . Therefore, E_{total} can be written as follows:

$$E_{total} = E_{gb} + W_{el} \quad (3)$$

As grain growth proceeds, the grain boundary energy reduces due to the decrease of the grain boundary area, whereas elastic strain increases because of accumulated stress and strain in the film.

The grain boundary energy is given by [22, 25]:

$$E_{gb} = \frac{\beta}{L} \gamma \quad (4)$$

where γ is the grain boundary energy per unit area, L is the average grain size, and β is the geometrical factor determined by the shape of the grains. β has a value of 2 if grains have a square cross section, a value of 3 for grains with a circular cross section and amounts to $4/\sqrt{3}$ for grains with a hexagonal cross section [22, 25, 26].

The strain energy, which is associated with stress, is given by [25]

$$W_{el} = \frac{1}{2} \sigma_{xx} \epsilon_{xx} + \frac{1}{2} \sigma_{yy} \epsilon_{yy} \quad (5)$$

Using Using Hook's law, this becomes

$$W_{el} = \left(\frac{E}{1-v} \right) \epsilon^2 = \left(\frac{E}{1-v} \right) \frac{(\alpha a)^2}{4} \left(\frac{1}{L_0} - \frac{1}{L} \right)^2 \quad (6)$$

Therefore,

$$E_{total} = \frac{\beta}{L} \gamma + \left(\frac{E}{1-v} \right) \frac{(\alpha a)^2}{4} \left(\frac{1}{L_0} - \frac{1}{L} \right)^2 \quad (7)$$

An infinitesimal amount of grain growth dL produces an energy change given by

$$dE = -\frac{\beta \gamma}{L^2} dL - \left(\frac{E}{1-v} \right) \frac{(\alpha a)^2}{2L^2} \left(\frac{1}{L} - \frac{1}{L_0} \right) dL \quad (8)$$

This energy variation is equal to that generated by the migration of grain boundaries in response to a driving pressure difference ΔP .

$$dE = -\Delta P \frac{\beta}{L} \frac{dL}{2} \quad (9)$$

Combining (8) and (9) results in,

$$\Delta P = \frac{2\gamma}{L} + \left(\frac{E}{1-v} \right) \frac{(\alpha a)^2}{\beta L} \left(\frac{1}{L} - \frac{1}{L_0} \right) \quad (10)$$

Following expressions given by Shewmon [27] and Smith [28], the rate of grain growth as a velocity is given by

$$\frac{dL}{dt} = \frac{D^* Q}{kT\delta} \Delta P \quad (11)$$

where D^* is the diffusivity given by $D_0 \exp(-E_a/kT)$, D_0 is the pre-exponential factor for grain boundary diffusion, E_a is the activation energy of grain boundary diffusion, Ω is the atomic volume, δ is the average jump distance in the grain boundary, k is the Boltzmann constant, and T is the absolute temperature.

Finally, the kinetics of grain growth can be derived by combining (10) and (11).

$$\frac{dL}{dt} = \frac{D^* \Omega}{kT\delta} \frac{2\gamma}{L} \left(I - \left(\frac{E}{1-v} \right) \frac{(\alpha a)^2}{2\beta\gamma} \left(\frac{1}{L_0} - \frac{1}{L} \right) \right) \quad (12)$$

As mentioned in section II, grain size can be determined by using linear intercept method. Based on the FIB images of 3 and 8 μm thick Cu films which were taken at 2h, 20h and 44h, the grain sizes have been extracted and plotted as the dots in Fig. 4. It exhibits that both films undergo a continuous increase of grain size during the whole measurement period. Meanwhile, the simulated curves of 3 and 8 μm thick Cu films are also plotted in Fig. 4 by the deduced differential equation (12). The grain sizes of 105 and 135nm accordingly obtained from FIB images of 3 and 8 μm thick Cu films are applied as original grain size L_0 in the simulation. As a consequence, the simulated curves converge with the experimental data very well.

By the incorporation of the grain growth rate model (12) into the grain growth model (2), we obtain the direct relationship between stress increased due to grain growth and time. Thus, stress increase as a function of time can be plotted as in Fig. 5. The modeled stress curves display for both films the stagnation after $\sim 1500\text{min}$, though the grain size still continuously dramatically increases as shown in Fig. 4. This indicates that the grain growth from fine grains to moderate grains contributes the major part to the stress increase. Later on, the grain growth from moderate grains to coarse grains only plays a minor role in stress increase. As a result, it shows clearly that stress increase due to grain growth is film thickness/grain size dependent. 3 μm thick Cu films have a

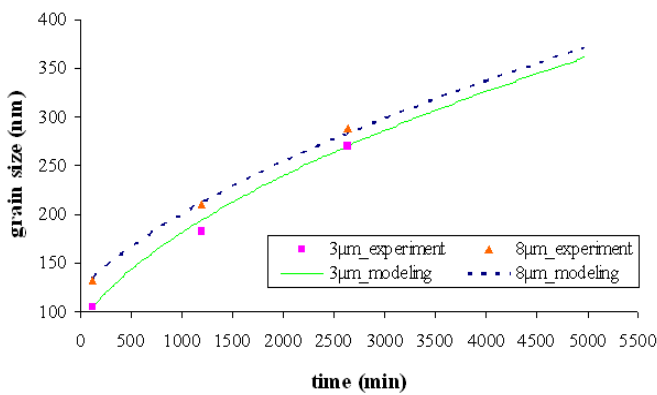


Figure 4. Grain size development of 3 and 8 μm thick ECD Cu films at room temperature. The modeled curves are in good agreement with the experimental data (markers) which is determined from FIB images. The following material properties are used in the simulation: $E_a = 1.46 \times 10^{-19} \text{ J}$, $D_0 = 3.04 \times 10^{-5} \text{ m}^2/\text{s}$, $\Omega = 1.182 \times 10^{-29} \text{ m}^3$, $\gamma = 0.625 \text{ J/m}^2$, $\delta = 0.40486 \text{ nm}$, $\beta = 2$.

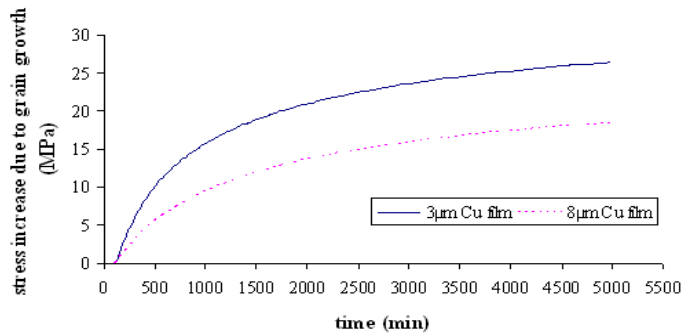


Figure 5. Stress increase of 3 and 8 μm thick ECD Cu films as function of time induced by grain boundary loss due to grain growth.

stress increase of $\sim 27\text{MPa}$ compared to $\sim 18\text{MPa}$ in 8 μm thick films. This is due to the fact that original grain size is smaller in thinner films. As the amount of stress increase is mainly determined by the fine grains, a smaller original grain size will result in a larger stress increase.

C. Grain boundary strengthening to dislocation plasticity

At room temperature, grain boundaries as well as dislocations act as obstacles to dislocation motion. Impeding the dislocation motion will hinder the onset of plasticity and hence increase the yield strength of the film. The dislocation pileup which determines the stress concentration in the grains, relates to the grain diameter and dislocation density. If the grain size is large and dislocation density is high, a greater stress concentration is developed in the grains, and thus the applied stress needed to activate plastic flow in the grains is relatively low, and vice versa. Hall-Petch law well represents the grain boundary barrier to dislocation motion as function of grain size [8, 29-31]. By the modified Hall-Petch equation the stress decrease due to dislocation motion can be calculated:

$$\Delta\sigma_{gb} = \sigma_L - \sigma_{L_0} = K \left(\frac{1}{\sqrt{L}} - \frac{1}{\sqrt{L_0}} \right) \quad (13)$$

where $\Delta\sigma_{gb}$ is the stress change due to dislocation glide, σ_L and σ_{L_0} are the flow stress of the film in the case of the grain size of L and L_0 , respectively, K is the Hall-Petch coefficient.

If the grain growth rate model (12) is incorporated into Hall-Petch equation (13), the direct relationship between stress decrease by dislocation glide and time is obtained and shown in Fig. 6. As discussed in section II, in thick Cu films (8-20 μm) dislocation plasticity can only be activated if a certain value of the threshold stress is reached. Therefore, according to the experimental data in Fig. 1, it is assumed that dislocation plasticity in 8 μm thick Cu films is activated when grain growth reaches the grain size of $\sim 190\text{nm}$ after 820min. Similar to the stress increase by grain growth, the stress decrease due to dislocation plasticity is film thickness/grain size dependent as well. It indicates that thicker films end up with less stress relaxation, which explains why stress decrease becomes less prominent with the increasing film thickness. The stress decrease tendency is even not visible in 20 μm thick Cu film, because dislocation plasticity is so marginal that it is

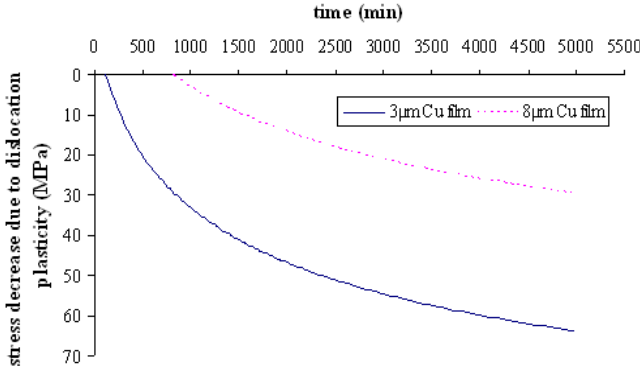


Figure 6. Stress decrease of 3 μm and 8 μm thick ECD Cu films induced by grain boundary strengthened dislocation plasticity. Note that for thick Cu films, e.g. 8 μm , dislocation motion doesn't start immediately after deposition, but only at 820min after deposition.

compensated by grain growth easily.

The Hall-Petch coefficient K reflects the resistance of grain boundaries to dislocation motion. Typically, a lower value of K refers to less resistance of dislocation motion, and vice versa. In Fig. 6, the modeled curves are calculated with the K value of 0.0448 MN/m $^{3/2}$, which is ~40% of the well-known Hall-Petch constant 0.112 MN/m $^{3/2}$ for face-centered cubic (FCC) copper [31]. During the abnormal grain growth, subgrains with low angle grain boundaries (<15°) may be strongly involved in the coarse-grained structure, which weakens the blocking of dislocations compared to high angle grain boundaries (>15°C)[32-34]. Consequently, Hall-Petch coefficient related to subgrains is typically 1/2 to 1/5 of the well-known value [31]. In order to capture the process of subgrain coarsening, in-situ electron backscatter diffraction (EBSD) or transmission electron microscopy (TEM) during grain growth would be required.

D. Model with competing mechanisms

As aforementioned, the individual mechanism of grain growth or dislocation plasticity does not enable us to interpret the complex stress evolution of ECD Cu films. Instead, a competing model combining the above two mechanisms, as shown in (14), needs to be applied in combination with grain growth rate model (12).

$$\sigma = \sigma_0 + \Delta\sigma_{gg} + \Delta\sigma_{gb} \quad (14)$$

where σ is the film stress, σ_0 is the as-deposited stress, $\Delta\sigma_{gg}$ and $\Delta\sigma_{gb}$ is the stress change due to grain growth and dislocation glide, respectively.

Fig. 7 shows the results of two representative numerical calculations in comparison with the corresponding experimental data labeled as dots. The as-deposited stress σ_0 is 60 MPa and 23 MPa for 3 μm and 8 μm thick Cu films, respectively. In Fig. 7, both calculated curves are qualitatively similar to the measured stress plots. As dislocation glide is prominent in the Cu films (1.5-5 μm), continuous

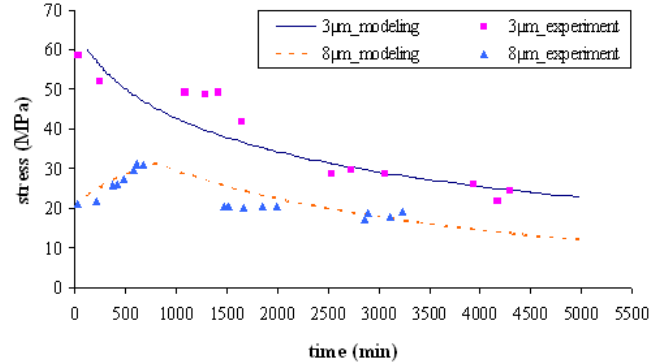


Figure 7. Experimental and modeled stress evolution of 3 and 8 μm thick ECD Cu films

decrease of stress, which is fully represented by the calculated curve of 3 μm thick Cu films, can be obtained by the described model with competing mechanisms. Meanwhile, the curve of 8 μm thick Cu films is well on the behalf of thicker films (8-20 μm), which conforms to grain growth and successive dislocation glide mechanisms.

However, there is a notable limitation of the model, which is associated with incubation of grain growth. As observed in Fig. 1, particularly in the stress evolution curves of thick Cu films (8-20 μm), stress increase does not start immediately after deposition, but at ~200min after the deposition. This implies that the onset of grain growth is retarded and all fine grains maintain as-deposited undergoing an incubation phase. The incubation of grain growth is not considered in the present model. Thus, the simulated results only emphasize on the stress evolution after the commencement of grain growth, but neglect the stress stabilization during incubation. Nevertheless, compared to the total evolution time, the incubation time is relatively short.

IV. CONCLUSION

A model with competing mechanisms has been developed to simulate the stress evolution of ECD Cu films. The model is based on the mechanisms of grain growth and dislocation plasticity. On the one hand, the stress increase is modeled by the loss of grain boundary volume due to grain growth. On the other hand, dislocation glide is responsible for the stress decrease. The incorporation of the model of grain size development makes it possible to include the time as a parameter into the competing model. The results show an accurate correlation between experimental data and simulated values. To extend the model, incubation phase of grain growth may be considered. Further, EBSD or TEM for the investigation of subgrains is required in order to determine important model parameters, such as the Hall-Petch coefficient.

ACKNOWLEDGMENT

The authors would like to thank M. Roemet for FIB measurements. Furthermore, Prof. G. Dehm is acknowledged with gratitude for many helpful discussions.

REFERENCES

- [1] M. D. Thouless, J. Gupta, and J. M. E. Harper, "Stress Development and Relaxation in Copper-Films During Thermal Cycling," *Journal of Materials Research*, vol. 8, pp. 1845-1852, Aug 1993.
- [2] L. T. Romankiw, "A path: from electroplating through lithographic masks in electronics to LIGA in MEMS," *Electrochimica Acta*, vol. 42, pp. 2985-3005, 1997.
- [3] P. C. Andricacos, C. Uzoh, J. O. Dukovic, J. Horkans, and H. Deligianni, "Damascene copper electroplating for chip interconnections," *IBM JOURNAL OF RESEARCH AND DEVELOPMENT*, vol. 42, pp. 567-574, 1998.
- [4] W. Robl, M. Melzl, B. Weidgans, R. Hofmann, and M. Stecher, "Last Metal Copper Metallization for Power Devices," in *IEEE Transactions on Semiconductor Manufacturing*, 2008, pp. 358-362.
- [5] K. Pantleon and M. A. J. Somers, "In situ investigation of the microstructure evolution in nanocrystalline copper electrodeposits at room temperature," *Journal of Applied Physics*, vol. 100, Dec 2006.
- [6] C. Lingk and M. E. Gross, "Recrystallization kinetics of electroplated Cu in damascene trenches at room temperature," *Journal of Applied Physics*, vol. 84, pp. 5547-5553, Nov 1998.
- [7] S. H. Brongersma, E. Richard, I. Vervoort, H. Bender, W. Vandervorst, S. Lagrange, G. Beyer, and K. Maex, "Two-step room temperature grain growth in electroplated copper," *Journal of Applied Physics*, vol. 86, p. 3642, 1999.
- [8] J. M. E. Harper, C. Cabral Jr, P. C. Andricacos, L. Gignac, I. C. Noyan, K. P. Rodbell, and C. K. Hu, "Mechanisms for microstructure evolution in electroplated copper thin films near room temperature," *Journal of Applied Physics*, vol. 86, pp. 2516-2525, 1999.
- [9] C. H. Seah, G. Z. You, C. Y. Li, and R. Kumar, "Characterization of electroplated copper films for three-dimensional advanced packaging," *Journal of Vacuum Science & Technology B*, vol. 22, pp. 1108-1113, May-Jun 2004.
- [10] W. H. Teh, L. T. Koh, S. M. Chen, J. Xie, C. Y. Li, and P. D. Foo, "Study of microstructure and resistivity evolution for electroplated copper films at near-room temperature," *Microelectronics Journal*, vol. 32, pp. 579-585, 2001.
- [11] V. A. Vas'ko, I. Tabakovic, S. C. Riemer, and M. T. Kief, "Effect of organic additives on structure, resistivity, and room-temperature recrystallization of electrodeposited copper," *Microelectronic engineering*, vol. 75, pp. 71-77, 2004.
- [12] V. Wehnacht and W. Brückner, "Abnormal grain growth in {111} textured Cu thin films," *Journal of Applied Physics*, vol. 418, pp. 136-144, 2002.
- [13] S. P. Hau-Riege and C. V. Thompson, "In situ transmission electron microscope studies of the kinetics of abnormal grain growth in electroplated copper films," *Applied Physics Letters*, vol. 76, pp. 309-311, Jan 2000.
- [14] M. T. Pérez-Prado and J. J. Vlassak, "Microstructural evolution in electroplated Cu thin films," *Journal of Applied Physics*, vol. 47, pp. 817-823, 2002.
- [15] Q. T. Jiang and M. E. Thomas, "Recrystallization effects in Cu electrodeposits used in fine line damascene structures," *Journal of Vacuum Science & Technology B: Microelectronics and Nanometer Structures*, vol. 19, pp. 762-766, 2001.
- [16] K. B. Yin, Y. D. Xia, C. Y. Chan, W. Q. Zhang, Q. J. Wang, X. N. Zhao, A. D. Li, Z. G. Liu, M. W. Bayes, and K. W. Yee, "The kinetics and mechanism of room-temperature microstructural evolution in electroplated copper foils," *Scripta Materialia*, vol. 58, pp. 65-68, 2008.
- [17] K. B. Yin, Y. D. Xia, W. Q. Zhang, Q. J. Wang, X. N. Zhao, A. D. Li, Z. G. Liu, X. P. Hao, L. Wei, C. Y. Chan, K. L. Cheung, M. W. Bayes, and K. W. Yee, "Room-temperature microstructural evolution of electroplated Cu studied by focused ion beam and positron annihilation lifetime spectroscopy," *Journal of Applied Physics*, vol. 103, pp. 066103-3, 2008.
- [18] H. Lee, W. D. Nix, and S. S. Wong, "Studies of the driving force for room-temperature microstructure evolution in electroplated copper films," *Journal of Vacuum Science & Technology B*, vol. 22, pp. 2369-2374, Sep-Oct 2004.
- [19] W. Zhang, S. H. Brongersma, Z. Li, D. Li, O. Richard, and K. Maex, "Analysis of the size effect in electroplated fine copper wires and a realistic assessment to model copper resistivity," vol. 101: *Journal of applied physics*, 2007, p. 063703.
- [20] M. Stangl and M. Militzer, "Modeling self-annealing kinetics in electroplated Cu thin films," in *JOURNAL OF APPLIED PHYSICS* vol. 103: AIP, 2008, p. 113521.
- [21] R. Huang, "Stress, sheet resistance and microstructure evolution of electroplated Cu films during self-annealing," *IEEE transactions on device and materials reliability*, accepted, 2009.
- [22] P. Chaudhari, "Grain Growth and Stress Relief in Thin Films," in *Journal of Vacuum Science and Technology*. vol. 9, 1972, pp. 520-522.
- [23] H. Lee, S. S. Wong, and S. D. Lopatin, "Correlation of stress and texture evolution during self- and thermal annealing of electroplated Cu films," *Journal of Applied Physics*, vol. 93, pp. 3796-3804, Apr 2003.
- [24] C. Cabral, P. C. Andricacos, L. Gignac, I. C. Noyan, K. P. Rodbell, T. M. Shaw, R. Rosenberg, J. M. E. Harper, P. W. DeHaven, and P. S. Locke, "Room temperature evolution of microstructure and resistivity in electroplated copper films," in *Advanced Metallization Conference*, Colorado, 1998, p. 81.
- [25] M. F. Doerner and W. D. Nix, "Stresses and deformation processes in thin films on substrates," *Critical Reviews in Solid State and Materials Sciences*, vol. 14, pp. 225-268, 1988.
- [26] Q. Z. Hong, J. M. E. Harper, and S. Q. Hong, "Stresses and morphological instabilities in silicide/polycrystalline Si layered structures," vol. 62, 1993, p. 2637.
- [27] P. G. Shewmon, *Transformations in Metals*. New York: McGraw-Hill, 1969.
- [28] C. M. F. Rae and D. A. Smith, "On the Mechanisms of Grain-Boundary Migration," *Philosophical Magazine a-Physics of Condensed Matter Structure Defects and Mechanical Properties*, vol. 41, pp. 477-492, 1980.
- [29] R. Venkatraman and J. C. Bravman, "Separation of film thickness and grain boundary strengthening effects in Al thin films on Si," in *Journal of Materials Research*. vol. 7, 1992, pp. 2040-2048.

- [30] R. M. Keller, S. P. Baker, and E. Arzt, "Quantitative analysis of strengthening mechanisms in thin Cu films: Effects of film thickness, grain size, and passivation," in *Journal of Materials Research*, vol. 13: Pittsburgh, PA: Published for the Materials Research Society by the American Institute of Physics, c1986-, 1998, pp. 1307-1317.
- [31] T. H. Courtney and T. Hugh, *Mechanical behavior of materials*. New York McGraw-Hill New York, 1990.
- [32] F. J. Humphreys, "A unified theory of recovery, recrystallization and grain growth, based on the stability and growth of cellular microstructures--I. The basic model," *Acta Materialia*, vol. 45, pp. 4231-4240, 1997.
- [33] E. A. Holm, M. A. Miodownik, and A. D. Rollett, "On abnormal subgrain growth and the origin of recrystallization nuclei," *Acta Materialia*, vol. 51, pp. 2701-2716, 2003.
- [34] W. Blum and X. H. Zeng, "A simple dislocation model of deformation resistance of ultrafine-grained materials explaining Hall-Petch strengthening and enhanced strain rate sensitivity," *Acta Materialia*, vol. 57, pp. 1966-1974, 2009.